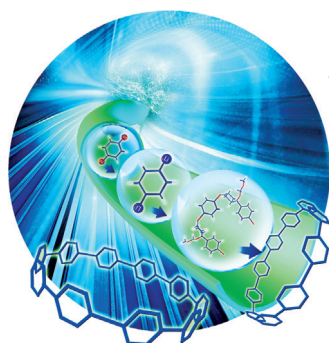
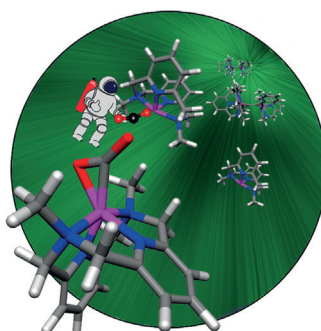


... through metal–ligand bifunctional catalysis or cooperative catalysis is like dancing the tango. In their Communication on page 1523 ff., A. Gansäuer and co-workers show that amides can be activated for radical reduction by amide-substituted titanocene(III) catalysts or through cooperative catalysis with titanocenes and Crabtree's catalyst (graphic design by Dina Schwarz G. Henriques).

CO₂ Activation

The activation of CO₂ by a cationic mononuclear nickel(I) complex is described by M. A. Johnson et al. in their Communication on page 1282 ff. The resulting complex features a bent CO₂ molecule (148°) bound to the metal center in an η² arrangement.

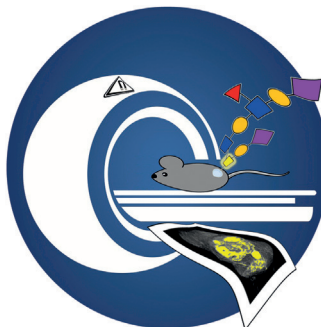


Microreactors

In their Communication on page 1422 ff., D.-P. Kim and co-workers describe a flow-assisted system for the efficient synthesis of the cycloparaphenylene (CPP) derivative [10]CPP under mild reaction conditions.

Magnetic Resonance Imaging

The imaging of cell-surface glycans in live mice, following metabolic labeling and subsequent bio-orthogonal reaction, by magnetic resonance imaging is described by A. A. Neves et al. in their Communication on page 1286 ff.



How to contact us:

Editorial Office:

E-mail: angewandte@wiley-vch.de

Fax: (+49) 62 01–606-331

Telephone: (+49) 62 01–606-315

Reprints, E-Prints, Posters, Calendars:

Carmen Leitner

E-mail: chem-reprints@wiley-vch.de

Fax: (+49) 62 01–606-331

Telephone: (+49) 62 01–606-327

Copyright Permission:

Bettina Loycke

E-mail: rights-and-licences@wiley-vch.de

Fax: (+49) 62 01–606-332

Telephone: (+49) 62 01–606-280

Online Open:

Margitta Schmitt

E-mail: angewandte@wiley-vch.de

Fax: (+49) 62 01–606-331

Telephone: (+49) 62 01–606-315

Subscriptions:

www.wileycustomerhelp.com

Fax: (+49) 62 01–606-184

Telephone: 0800 1800536 (Germany only)
+44(0) 1865476721 (all other countries)

Advertising:

Marion Schulz

E-mail: mschulz@wiley-vch.de

Fax: (+49) 62 01–606-550

Telephone: (+49) 62 01–606-565

Courier Services:

Boschstrasse 12, 69469 Weinheim

Regular Mail:

Postfach 101161, 69451 Weinheim

Angewandte Chemie International Edition is a journal of the Gesellschaft Deutscher Chemiker (GDCh), the largest chemistry-related scientific society in continental Europe. Information on the various activities and services of the GDCh, for example, cheaper subscription to *Angewandte Chemie International Edition*, as well as applications for membership can be found at www.gdch.de or can be requested from GDCh, Postfach 900440, D-60444 Frankfurt am Main, Germany.

GDCh

GESELLSCHAFT
DEUTSCHER CHEMIKER

Get the **Angewandte App**
International EditionAvailable on the
App Store**Enjoy Easy Browsing and a New Reading Experience on the iPad or iPhone**

- Keep up to date with the latest articles in Early View.
- Download new weekly issues automatically when they are published.
- Read new or favorite articles anytime, anywhere.



"... Solvents are often considered to be an inert media, in which reactions occur. A molecular-level, bottom-up description of solvation that is able to predict the properties of new solvent systems, also for industrial applications has come within reach. Solvents are now increasingly recognized as playing an active role in their own right in various processes ..."

Read more in the Editorial by Martina Havenith.

Editorial

M. Havenith-Newen* — 1218–1219

Solvation Science: A New Interdisciplinary Field

Spotlight on Angewandte's Sister Journals

1240–1243

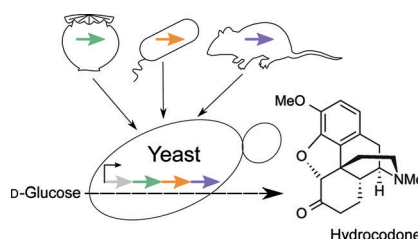


"My biggest motivation is unexpected results. I lose track of time when I am doing experiments ..."
This and more about Akira Harada can be found on page 1244.

Service**Author Profile**

Akira Harada — 1244

Home brew: Biotechnological modification of the yeast *Sacharomyces cerevisiae* enabled the production of opioids from glucose. This challenging extension of yeast metabolism, the result of ten years of work, involves the artificial expression of 23 genes originating from yeast, plants, and rats. This breakthrough was achieved by applying the design principles of synthetic biology, systems biology, and protein engineering.

**Highlights****Synthetic Biology**

M. Höhne, J. Kabisch* — 1248–1250

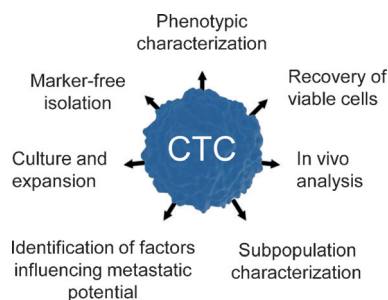
Brewing Painkillers: A Yeast Cell Factory for the Production of Opioids from Sugar

Minireviews

Tumor Profiling

B. J. Green, T. Saberi Safaei, A. Mephram,
M. Labib, R. M. Mohamadi,
S. O. Kelley* ————— 1252 – 1265

Beyond the Capture of Circulating Tumor Cells: Next-Generation Devices and Materials



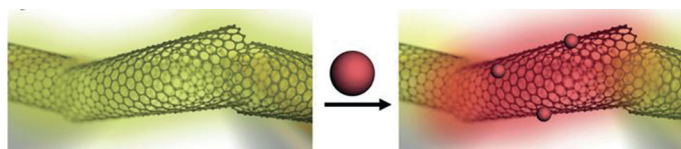
Deadliest catch: Over the last decade, significant progress has been made towards the capture of rare circulating tumor cells (CTCs) from the blood of cancer patients, a critical capability for noninvasive tumor profiling. This Minireview summarizes recent breakthroughs and focuses on how new devices and materials have allowed this rapidly advancing field to move beyond enumeration and towards comprehensive characterization of CTCs.

Reviews

Sensors

J. F. Fennell, Jr., S. F. Liu, J. M. Azzarelli,
J. G. Weis, S. Rochat, K. A. Mirica,
J. B. Ravnsbæk,
T. M. Swager* ————— 1266 – 1281

Nanowire Chemical/Biological Sensors: Status and a Roadmap for the Future



Down to the wire: Sensors based on chemiresistance can be readily integrated into electronic devices and are low priced compared to conventional analytical devices. This Review illustrates the

advantages of such sensors, which transduce the binding or action of an analyte on a nanowire or nanowire arrangement into a signal.

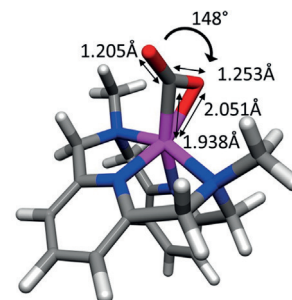
Communications

CO₂ Activation

F. S. Menges, S. M. Craig, N. Tötsch,
A. Bloomfield, S. Ghosh, H.-J. Krüger,
M. A. Johnson* ————— 1282 – 1285

Capture of CO₂ by a Cationic Nickel(I) Complex in the Gas Phase and Characterization of the Bound, Activated CO₂ Molecule by Cryogenic Ion Vibrational Predissociation Spectroscopy

Highly distorted: A CO₂ molecule is activated in the gas phase by a cationic mononuclear nickel(I) complex containing a tetraazamacrocyclic ligand. The resulting complex was structurally characterized by mass-selected vibrational predissociation spectroscopy, which indicated that this complex features a highly distorted CO₂ molecule bound to the metal center in an η^2 -C,O coordination mode.



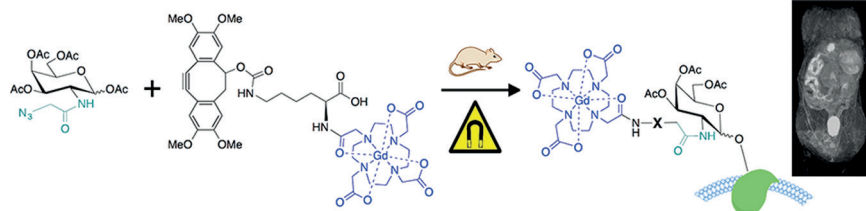
Frontispiece

For the USA and Canada:

ANGEWANDTE CHEMIE International Edition (ISSN 1433-7851) is published weekly by Wiley-VCH, PO Box 101161, 69451 Weinheim, Germany. US mailing agent: SPP, PO Box 437, Emigsville, PA 17318. Periodicals postage

paid at Emigsville, PA. US POSTMASTER: send address changes to *Angewandte Chemie*, John Wiley & Sons Inc., C/O The Sheridan Press, PO Box 465, Hanover, PA 17331. Annual subscription price for institutions: US\$ 16.862/14.051 (valid for print and electronic / print or

electronic delivery); for individuals who are personal members of a national chemical society prices are available on request. Postage and handling charges included. All prices are subject to local VAT/sales tax.



Glycans were imaged in live mice by magnetic resonance imaging, following metabolic labeling with an azido sugar and subsequent administration of a strained cyclooctyne linked to a gadoli-

nium contrast agent. Significant azido sugar dependent contrast was observed in various tissues two hours after administration of the contrast agent.

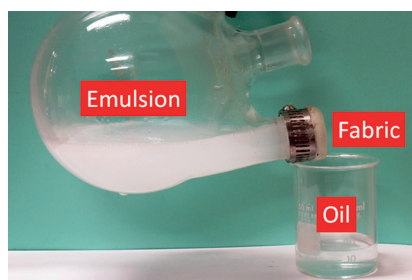
Magnetic Resonance Imaging

A. A. Neves,* Y. A. Wainman, A. Wright, M. I. Kettunen, T. B. Rodrigues, S. McGuire, D.-E. Hu, F. Bulat, S. Geninatti Crich, H. Stöckmann, F. J. Leeper, K. M. Brindle — **1286–1290**

Imaging Glycosylation In Vivo by Metabolic Labeling and Magnetic Resonance Imaging

Back Cover

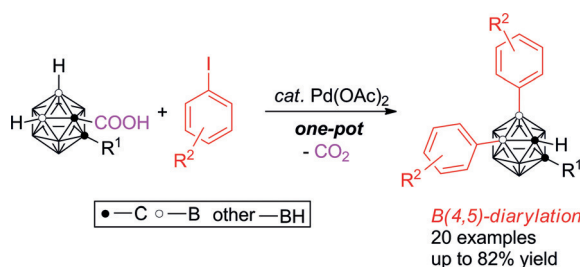
A superhydrophobic and a polyamine-bearing surface make up a Janus cotton fabric. When used as a filter, the polyamine-bearing side causes micrometer-sized oil droplets to coalesce and the hydrophobic side allows selective oil permeation. Oil separation using this method is rapid and the separated oil is very pure: hexadecane content in water after a separation can be reduced to less than 0.03 ± 0.03 vol%.



Oil/Water Separation

Z. Wang, Y. Wang, G. Liu* — **1291–1294**

Rapid and Efficient Separation of Oil from Oil-in-Water Emulsions Using a Janus Cotton Fabric



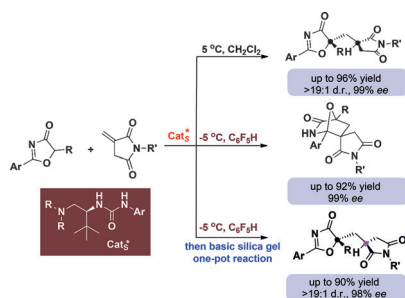
Palladium-catalyzed intermolecular coupling of *o*-carborane with aromatics by direct cage B–H bond activation has been achieved, leading to the synthesis of a series of cage B(4,5)-diarylated-*o*-car-

boranes in high yields with excellent regioselectivity. Traceless directing group -COOH plays a crucial role for site- and di-selectivity of such intermolecular coupling reactions.

Carborane Functionalization

Y. Quan, Z. Xie* — **1295–1298**

Palladium-Catalyzed Regioselective Diarylation of *o*-Carboranes By Direct Cage B–H Activation



Divergent reaction paths: The first asymmetric reaction of 5*H*-oxazol-4-ones with itaconimides was developed by employing a chiral tertiary amine–urea catalyst. The substrates could go through either tandem conjugate addition–protonation or [4+2] cycloaddition with excellent enantio- and diastereoselectivities under controlled experimental conditions.

Organocatalysis

B. Zhu, R. Lee, J. Li, X. Ye, S.-N. Hong, S. Qiu, M. L. Coote,*
Z. Jiang* — **1299–1303**

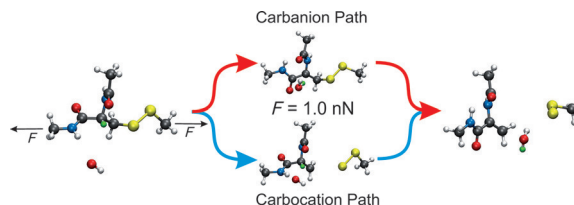
Chemoselective Switch in the Asymmetric Organocatalysis of 5*H*-Oxazol-4-ones and *N*-Itaconimides: Addition–Protonation or [4+2] Cycloaddition

Mechanochemistry

P. Dopieralski,* J. Ribas-Arino,*
P. Anjukandi, M. Krupicka,
D. Marx* 1304–1308



Force-Induced Reversal of β -Eliminations:
Stressed Disulfide Bonds in Alkaline
Solution



Mechanical stress influences the pathway of disulfide cleavage by β -elimination. The rate-determining first step, the abstraction of the β -proton, is insensitive to external forces. Forces larger than about

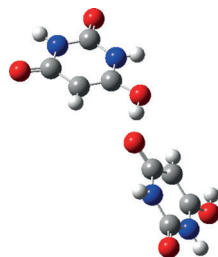
1 nN reshape the free-energy landscape so that the order of the reaction steps is reversed, turning β -deprotonation into a barrier-free follow-up process to C–S cleavage.

Polymorphism

M. G. Marshall, V. Lopez-Diaz,
B. S. Hudson* 1309–1312



Single-Crystal X-ray Diffraction Structure of the Stable Enol Tautomer Polymorph of Barbituric Acid at 224 and 95 K



Tautomer lesson: The enol polymorph of barbituric acid has been crystallized and its structure determined at 95 K (N blue, O red, C gray, H white). The tri-keto tautomer of barbituric acid in solution and by computation is more stable than the enol by about 50 kJ mol^{−1}. However, the enol is the stable tautomer. Replacement of the four H atoms by D reverses the order of the stability of the tautomers.

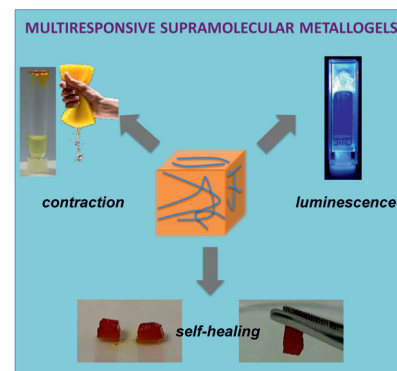
Supramolecular Metallogels

E. Borr , J.-F. Stumb ,
S. Bellemin-Laponnaz,*
M. Mauro* 1313–1317



Light-Powered Self-Healable
Metallosupramolecular Soft Actuators

Lights, camera, action! A series of metal-lolymers based on Zn^{II}–terpyridine coordination nodes and bearing photo-isomerizable and/or luminescent moieties are reported. The polymers undergo gelation at ultralow critical concentrations. The resulting multiresponsive organogels are photoluminescent, display light-triggered mechanical actuation, and can rapidly self-heal.

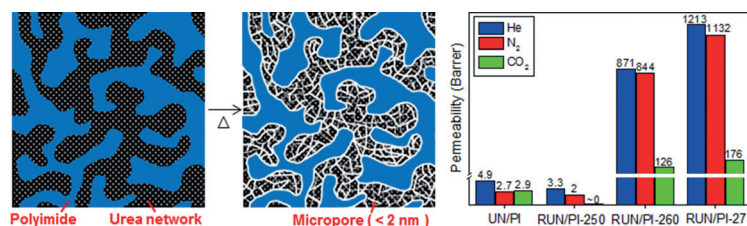


Microporous Membranes

E. Jeon, S.-Y. Moon, J.-S. Bae,
J.-W. Park* 1318–1323

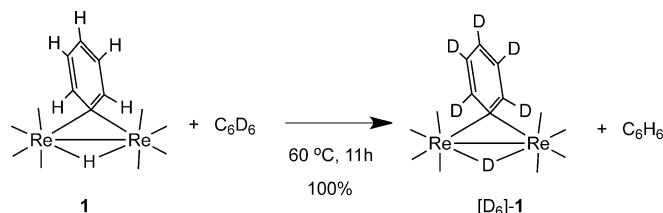


In situ Generation of Reticulate Micropores through Covalent Network/Polymer Nanocomposite Membranes for Reverse-Selective Separation of Carbon Dioxide



Selective networking: Reticular microporous channels are generated in situ throughout a urea-based network film by selective expulsion of molecular fragments during a thermal rearrangement.

The nanocomposite membranes exhibited unusual reverse-selective gas-transport properties, rejecting carbon dioxide while transporting different gases.



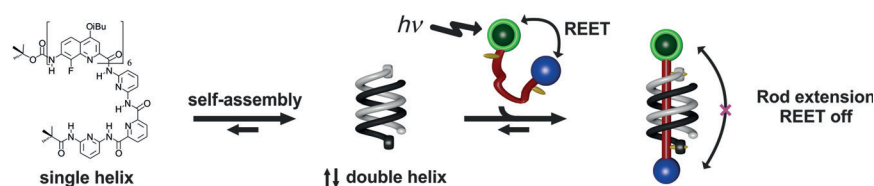
Two Rheniums are better than one: The electronically unsaturated dirhenium complex $[\text{Re}_2(\text{CO})_8(\mu\text{-H})(\mu\text{-Ph})]$ (**1**) exhibits aromatic C–H activation upon reaction with $[\text{D}_6]$ benzene to yield $[\text{D}_6]\text{-1}$ in good yield. The mechanism has been

elucidated by DFT analyses, and involves a binuclear C–H bond-activation process. *N,N*-Diethylaniline and naphthalene also react with **1** to generate $[\text{Re}_2(\text{CO})_8(\mu\text{-H})(\mu\text{-}\eta^1\text{-NEt}_2\text{C}_6\text{H}_4)]$ and $[\text{Re}_2(\text{CO})_8(\mu\text{-H})(\mu\text{-}\eta^2\text{-1,2-C}_{10}\text{H}_7)]$, respectively.

C–H Activation

R. D. Adams,* V. Rassolov,*
Y. O. Wong ————— **1324–1327**

Binuclear Aromatic C–H Bond Activation at a Dirhenium Site



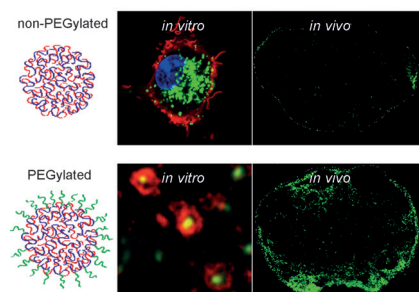
A supramolecular abiotic double helix interpenetrated by a bichromophoric thread is described. While reversible interchromophore electronic energy transfer occurs in the excited free thread, giving prolonged emission, luminescence

lifetime shortens when decoupled in the complex. The high sensitivity of emission decay to distance offers an approach to luminescence lifetime-based conformational probes.

Foldamers

S. A. Denisov, Q. Gan, X. Wang,
L. Scarpantonio, Y. Ferrand,*
B. Kauffmann, G. Jonusauskas, I. Huc,
N. D. McClenaghan* ————— **1328–1333**

Electronic Energy Transfer Modulation in a Dynamic Foldaxane: Proof-of-Principle of a Lifetime-Based Conformation Probe



Lymphatic transportation: PEGylation is shown to be a key parameter for lymphatic transportation of hydrogel nanoparticles. The PEGylated nanoparticles result in a high association with dendritic cells and B cells as well as increased T cell responses in vivo, which can be potentially used to improve the delivery of vaccines and drugs to the lymph nodes.

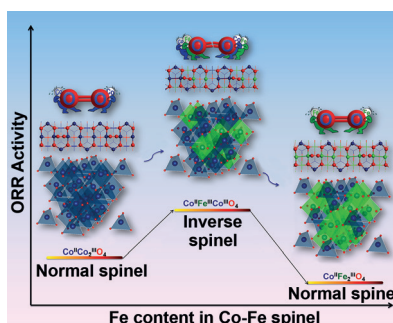
Drug Delivery

S. De Koker, J. Cui, N. Vanparijs,
L. Albertazzi, J. Grooten, F. Caruso,*
B. G. De Geest* ————— **1334–1339**

Engineering Polymer Hydrogel Nanoparticles for Lymph Node-Targeted Delivery



Enhancing by reversing: The electrocatalytic performance of Co-Fe based spinel for the oxygen reduction reaction can be significantly promoted by reversing its structure from normal to inverse. The enhancement of activity originates from a dissimilarity effect of Fe and Co atoms at the octahedral sites, which modulates the oxygen adsorption energy (E_{ad}) and elongates the O–O bond compared to that on the normal spinel.



Electrocatalysis

G. Wu, J. Wang, W. Ding,* Y. Nie, L. Li,*
X. Qi, S. Chen, Z. Wei* ————— **1340–1344**

A Strategy to Promote the Electrocatalytic Activity of Spinel for Oxygen Reduction by Structure Reversal



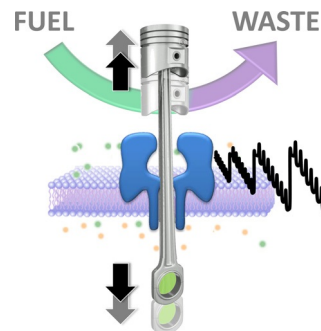
**Molecular Machines**

M. A. Watson,
S. L. Cockcroft* _____ **1345 – 1349**



An Autonomously Reciprocating
Transmembrane Nanoactuator

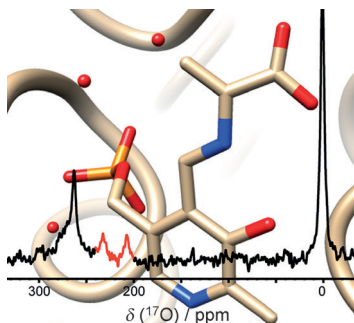
Machina trans membrana: A transmembrane nanoactuator turns over chemical fuel to drive autonomous nanomechanical motion. The ratcheted reciprocating motion of a DNA/PEG copolymer threaded through a single α -hemolysin pore was induced by a combination of DNA strand displacement processes and enzyme-catalyzed reactions.

**NMR Spectroscopy**

R. P. Young, B. G. Caulkins, D. Borchardt,
D. N. Bulloch, C. K. Larive, M. F. Dunn,
L. J. Mueller* _____ **1350 – 1354**



Solution-State ^{17}O Quadrupole Central-
Transition NMR Spectroscopy in the
Active Site of Tryptophan Synthase



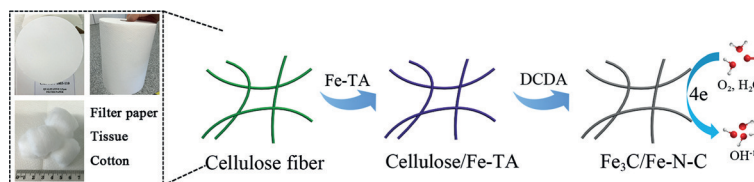
Enzymatic reactions: Several intermediates in the catalytic cycle of tryptophan synthase were characterized by ^{17}O quadrupole central-transition NMR spectroscopy. The picture shows the ^{17}O solution-state NMR spectrum of the kinetically competent α -aminoacrylate intermediate superimposed on the β -subunit active site.

**Oxygen-Reduction Reaction**

J. Wei, Y. Liang, Y. Hu, B. Kong,
G. P. Simon, J. Zhang, S. P. Jiang,
H. Wang* _____ **1355 – 1359**



A Versatile Iron–Tannin–Framework Ink
Coating Strategy to Fabricate Biomass-
Derived Iron Carbide/Fe–N–Carbon
Catalysts for Efficient Oxygen Reduction



Ink for a minute: A versatile iron–tannin–(TA)–framework “ink” coating strategy is demonstrated for the fabrication of high-performance $\text{Fe}_3\text{C}/\text{Fe-N-C}$ catalysts for the oxygen-reduction reaction (ORR) by using

low-cost, widely available, cellulose fiber-based materials (filter paper, tissue paper, and cotton), and even polyurethane-foam waste as the carbon source.

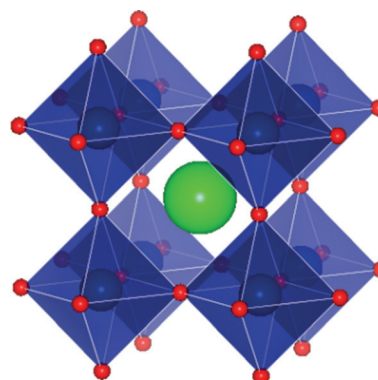
Perovskite Phases

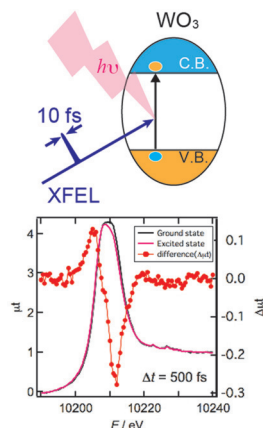
H. Seki, Y. Hosaka, T. Saito, M. Mizumaki,
Y. Shimakawa* _____ **1360 – 1363**



Ferromagnetism Induced by Substitution
of the Iron(IV) Ion by an Unusual High-
Valence Nickel(IV) Ion in
Antiferromagnetic SrFeO_3

Under pressure: Cubic perovskite derivatives $\text{SrFe}_{1-x}\text{Ni}_x\text{O}_3$ ($0 \leq x \leq 0.5$) with unusual high-valence Fe^{IV} and Ni^{IV} ions are obtained by high-pressure synthesis. In these compounds, the Ni^{IV} ion, which is intrinsically nonmagnetic, has a substantial magnetic moment, and ferromagnetism with a transition temperature (T_c) greater than room temperature is induced.



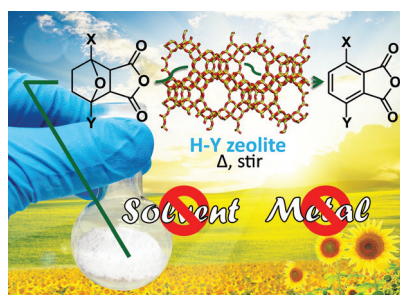


Caught on the “speed camera”: Photoexcited states of WO_3 were observed by femtosecond X-ray absorption spectroscopy performed using an X-ray free electron laser (XFEL). The local structural transformation of W was found, which occurred after the change of the local electronic state and began within 200 ps after excitation.

Photoexcitation

Y. Uemura, D. Kido, Y. Wakisaka, H. Uehara, T. Ohba, Y. Niwa, S. Nozawa, T. Sato, K. Ichihayashi, R. Fukaya, S.-i. Adachi, T. Katayama, T. Togashi, S. Owada, K. Ogawa, M. Yabashi, K. Hatada, S. Takakusagi, T. Yokoyama, B. Ohtani, K. Asakura* — **1364–1367**

Dynamics of Photoelectrons and Structural Changes of Tungsten Trioxide Observed by Femtosecond Transient XAFS

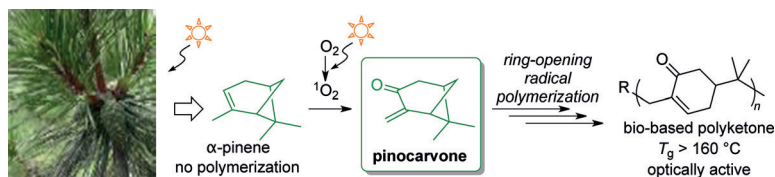


Just heat and tumble: Furanics-derived hydrogenated Diels-Alder adducts can be conveniently converted, over acidic zeolites, into renewable aromatics using a solid-phase conversion strategy. The zeolite H-Y was found to perform the best and can be easily reused after calcination.

Arenes

S. Thiagarajan, H. C. Genuino, J. C. van der Waal, E. de Jong,* B. M. Weckhuysen, J. van Haveren, P. C. A. Bruijninx,* D. S. van Es* — **1368–1371**

A Facile Solid-Phase Route to Renewable Aromatic Chemicals from Biobased Furanics



Polymers from α -pinene: The most abundant naturally occurring terpene, α -pinene, was quantitatively converted into pinocarvone, which contains a reactive *exo* methylene group, under visible-light irradiation. The bicyclic vinyl ketone

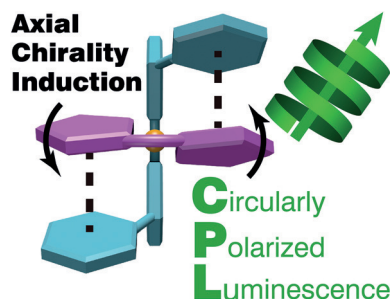
was quantitatively polymerized by selective ring-opening radical polymerization, resulting in novel bio-based polymers with good thermal properties, optical activities, and reactive groups.

Polymerization

H. Miyaji, K. Satoh,* M. Kamigaito* — **1372–1376**

Bio-Based Polyketones by Selective Ring-Opening Radical Polymerization of α -Pinene-Derived Pinocarvone

The odd couple: Heteroleptic zinc(II) complexes synthesized using achiral dipyrinato (shown in magenta) and chiral bis(oxazoline) ligands (turquoise) show bright fluorescence from the dipyrinato moiety with quantum efficiencies of up to 0.70. The luminescence is circularly polarized, which results from axial chirality induction to the dipyrinato ligand by the bis(oxazoline) ligand.



Photophysics

J. F. Kögel, S. Kusaka, R. Sakamoto,* T. Iwashima, M. Tsuchiya, R. Toyoda, R. Matsuoka, T. Tsukamoto, J. Yuasa,* Y. Kitagawa, T. Kawai,* H. Nishihara* — **1377–1381**

Heteroleptic [Bis(oxazoline)](dipyrinato)zinc(II) Complexes: Bright and Circularly Polarized Luminescence from an Originally Achiral Dipyrinato Ligand

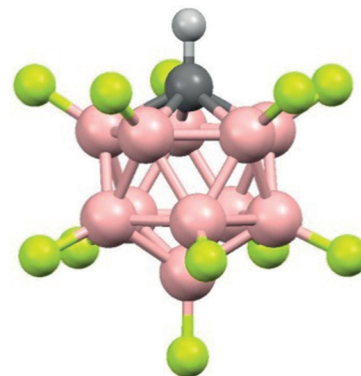
Superacids

S. Cummings, H. P. Hratchian,
C. A. Reed* — 1382 – 1386



The Strongest Acid: Protonation of
Carbon Dioxide

Acid test: The fluorinated carborane acid $\text{H}(\text{CHB}_{11}\text{F}_{11})$ protonates CO_2 forming the proton disolvate $\text{H}(\text{CO}_2)_2^+$. Traditional mixed superacids do not, so carborane acids are the strongest known acids.

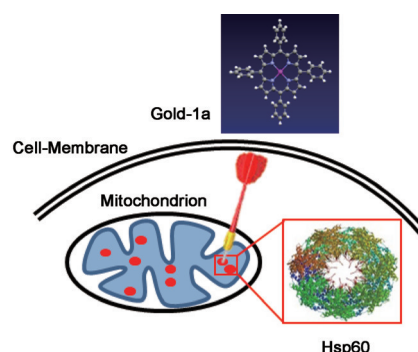


Metallo drugs

D. Hu, Y. Liu, Y.-T. Lai, K.-C. Tong,
Y.-M. Fung, C.-N. Lok,
C.-M. Che* — 1387 – 1391



Anticancer Gold(III) Porphyrins Target
Mitochondrial Chaperone Hsp60



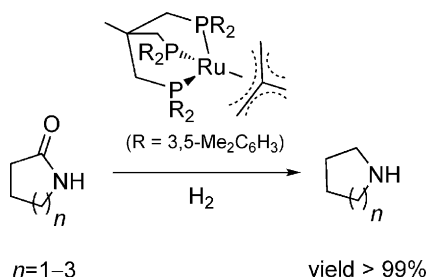
Golden gun: Hsp60 is a direct molecular target of the anticancer compound gold-(III) *meso*-tetraphenylporphyrin (**gold-1 a**) under both in vitro and cellular conditions, as revealed by chemical biology studies employing photo-affinity labeling, click chemistry, proteomic identification, cellular thermal shift, saturation-transfer difference NMR, protein fluorescence quenching, and protein chaperone assays.

Hydrogenation Catalysts

M. Meuresch, S. Westhues, W. Leitner,
J. Klankermayer* — 1392 – 1395



Tailor-Made Ruthenium-Triphos Catalysts
for the Selective Homogeneous
Hydrogenation of Lactams



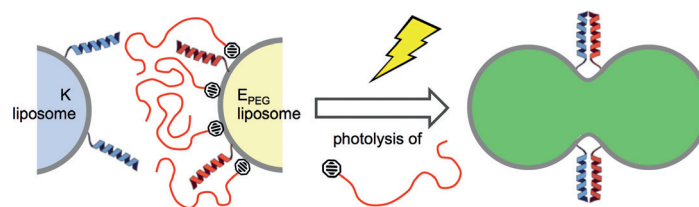
Bulky catalysts: A tailored sterically demanding tridentate ligand enabled the synthesis of a novel molecular ruthenium-triphos catalyst, which eliminates dimerization as the major deactivation pathway. The novel catalyst design showed increased performance and facilitated the hydrogenation of highly challenging lactam substrates with unprecedented activity and selectivity.

Photoactivation

L. Kong, S. H. C. Askes, S. Bonnet,
A. Kros,* F. Campbell* — 1396 – 1400

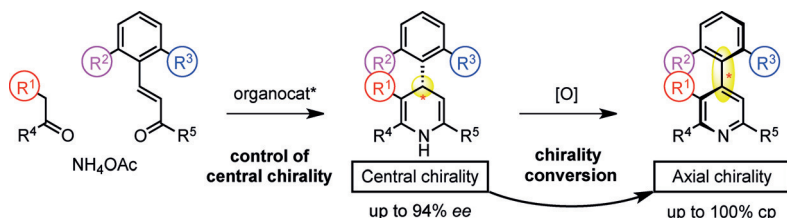


Temporal Control of Membrane Fusion
through Photolabile PEGylation of
Liposome Membranes



Membrane fusion was temporally controlled by photolabile steric shielding of fusogenic liposomes. An analogous method also enabled spatiotemporal control of liposome accumulation at cel-

lular membranes in vitro. This general approach represents a non-invasive, user-defined route towards vector-based drug and gene delivery both in vitro and in vivo.



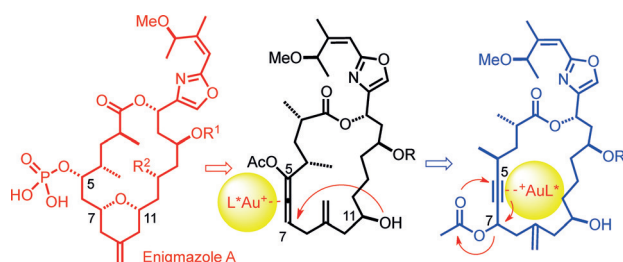
Enriched atropisomers: Substituted enantioenriched 4-aryl-1,4-dihydropyridines were prepared by an enantioselective Michael addition reaction, and then oxidized with MnO_2 into axially chiral 4-

arylpyridines with central-to-axial chirality conversion. Moderate to complete conversion percentages (cp) were observed, and a model for the conversion of chirality is discussed.

Enantioselective Reactions

O. Quinonero, M. Jean, N. Vanthuyne, C. Roussel, D. Bonne, T. Constantieux, C. Bressy,* X. Bugaut,* J. Rodriguez* 1401 – 1405

Combining Organocatalysis with Central-to-Axial Chirality Conversion: Atroposelective Hantzsch-Type Synthesis of 4-Arylpyridines



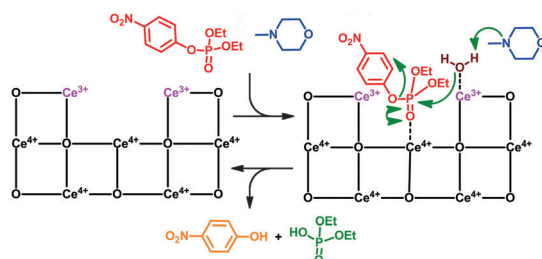
Within reach: A gold-catalyzed cascade of remarkable complexity paved the way to the parent phosphorylated macrolide of the enigmazole family, which exhibits a highly promising but not yet well-

understood biological profile. Only if the π -acid itself is chiral, however, was the [3,3]-sigmatropic rearrangement complete before the hydroxy group reached across the macrocyclic ring.

Natural Products

A. Ahlers, T. de Haro, B. Gabor, A. Fürstner* 1406 – 1411

Concise Total Synthesis of Enigmazole A



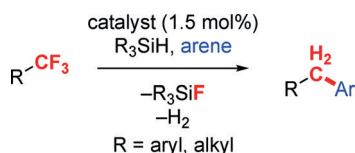
Catalytic hotspots: Vacancy-engineered cerium dioxide nanoparticles provide potential enzyme mimetic hotspots for the rapid degradation of nerve agents.

This study presents the first example of hydrolytic activity of a vacancy-engineered nanomaterial, where the dual oxidation states of the metal ions play a crucial role.

Nanocatalysis

A. A. Vernekar, T. Das, G. Mugesh* 1412 – 1416

Vacancy-Engineered Nanoceria: Enzyme Mimetic Hotspots for the Degradation of Nerve Agents



Do the job and get outta here! A range of arenes underwent benzylation or alkylation with trifluoromethyl-substituted aryl and alkyl substrates in the presence of the electrophilic organofluorophosphonium catalyst $[(\text{C}_6\text{F}_5)_3\text{PF}][\text{B}(\text{C}_6\text{F}_5)_4]$ and a silane. Hydrodefluorination occurred rapidly to complete the net transformation of the CF_3 group into a CH_2 -aryl fragment (see scheme).

Synthetic Methods

J. Zhu, M. Pérez, C. B. Caputo, D. W. Stephan* 1417 – 1421

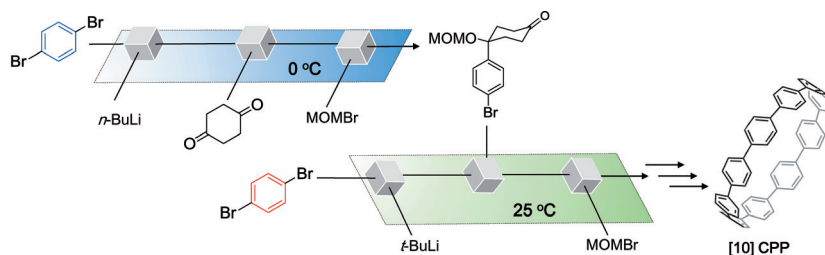
Use of Trifluoromethyl Groups for Catalytic Benzylation and Alkylation with Subsequent Hydrodefluorination

Microreactors

H. Kim, H.-J. Lee,
D.-P. Kim* 1422 – 1426



Flow-Assisted Synthesis of
[10]Cycloparaphenylene through Serial
Microreactions under Mild Conditions



Go with the flow: The cycloparaphenylene (CPP) derivative [10]CPP was synthesized in four steps under mild conditions using a flow-assisted synthetic method by precise control of the reaction time and flow

rate. Selective nucleophilic addition of a lithiated benzene derivative to a diketone could be achieved in high yield without a protection/deprotection step.

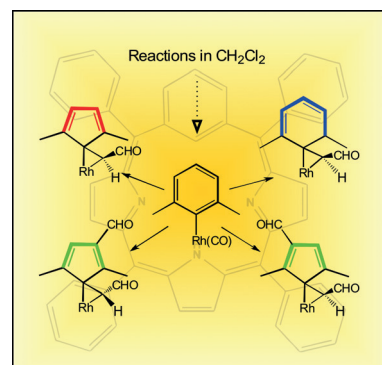
Porphyrins

K. Hurej, M. Pawlicki, L. Szterenber,
L. Latos-Grażyński* 1427 – 1431



A Rhodium-Mediated Contraction of
Benzene to Cyclopentadiene:
Transformations of Rhodium(III)
m-Benziporphyrin

Casting out a carbon: The *m*-phenylene ring in rhodium(III) *m*-benziporphyrin is demonstrated to undergo ring contraction to a cyclopentadienyl fragment, ultimately forming a unique rhodium(III) 21-carbaporphyrin derivative. The unusual coordination environment in this system facilitates the stabilization of peculiar structural motifs, specifically a rhoda-cyclopropane substituted by a formyl unit.

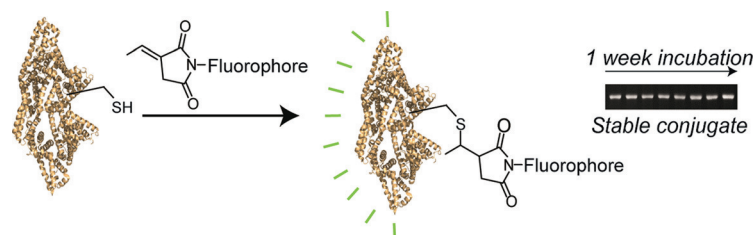


Bioconjugation

D. Kalia,* P. V. Malekar,
M. Parthasarathy 1432 – 1435



Exocyclic Olefinic Maleimides: Synthesis
and Application for Stable and Thiol-
Selective Bioconjugation



In stable bioconjugation: A variety of exocyclic olefinic maleimides have been prepared from endocyclic olefinic maleimides under solvent-free conditions by 4-nitrophenol-mediated catalysis. These scaffolds were found to react selectively

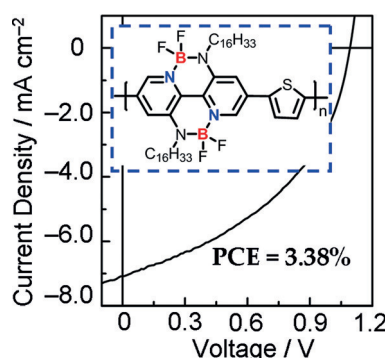
with thiols at physiological conditions to form linkages that resist thiol-exchange-mediated breakdown, thus demonstrating their potential for stable thiol bioconjugation.

Conjugated Polymers

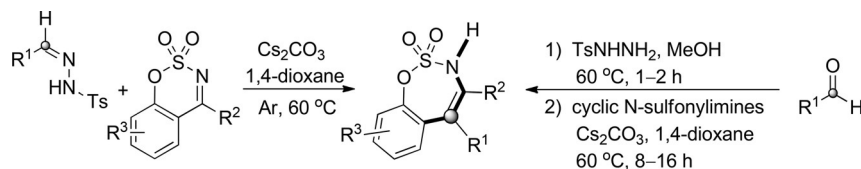
C. Dou, X. Long, Z. Ding, Z. Xie, J. Liu,*
L. Wang 1436 – 1440



An Electron-Deficient Building Block
Based on the B←N Unit: An Electron
Acceptor for All-Polymer Solar Cells



A bridge too far: An electron-deficient building block comprises a double B←N bridged bipyridyl (BNBP) moiety. The polymer constructed from the BNBP units exhibits high electron mobility, low-lying LUMO/HOMO energy levels, and strong absorbance in the visible range, and shows excellent device performance as polymer electron acceptor for all-polymer solar cells.



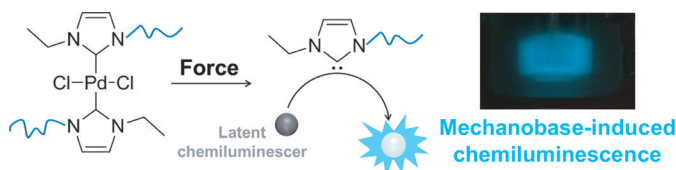
A diazo thing: The title reaction between cyclic N-sulfonylimines and diazo compounds generated in situ from the N-tosylhydrazones is simple and functional-group tolerant. It thus delivers valuable

seven-membered sulfonamides in up to 95% yield. Moreover, this reaction can be carried out in one-pot starting from the aryl aldehydes, without the need to isolate the N-tosylhydrazone (right).

Diazo Compounds

A.-J. Xia, T.-R. Kang,* L. He,* L.-M. Chen, W.-T. Li, J.-L. Yang,* Q.-Z. Liu* 1441–1444

Metal-Free Ring-Expansion Reaction of Six-membered Sulfonylimines with Diazomethanes: An Approach toward Seven-Membered Enesulfonamides



Mechanophores capable of releasing N-heterocyclic carbene are combined with triggerable chemiluminescent substrates to give a novel system for mechanically induced chemiluminescence. The mechanophores are palladium bis-NHC com-

plexes centrally incorporated in poly(tetrahydrofuran). Chemiluminescence is induced upon sonication of dilute solutions of the polymer complex and either APD or a coumaranone derivative.

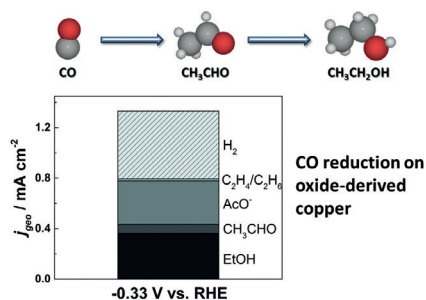
Mechanochemistry

J. M. Clough, A. Balan, T. L. J. van Daal, R. P. Sijbesma* 1445–1449

Probing Force with Mechanobase-Induced Chemiluminescence



An unappreciated intermediate: Acetaldehyde is identified as a product and key intermediate in CO reduction to ethanol on oxide-derived copper. It is also shown that the detection of acetaldehyde with NMR spectroscopy in alkaline solution is challenging, requiring utilization of complementary techniques.



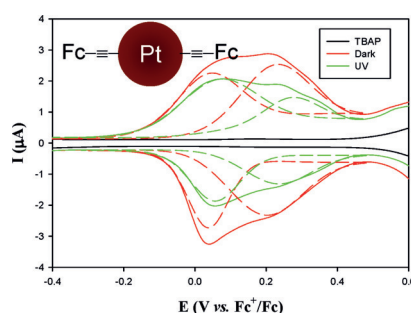
Electrochemistry

E. Bertheussen, A. Verdaguer-Casadevall, D. Ravasio, J. H. Montoya, D. B. Trimarco, C. Roy, S. Meier, J. Wendland, J. K. Nørskov, I. E. L. Stephens,* I. Chorkendorff* 1450–1454

Acetaldehyde as an Intermediate in the Electroreduction of Carbon Monoxide to Ethanol on Oxide-Derived Copper



UV photoirradiation leads to markedly enhanced intervalence charge transfer (IVCT) between ferrocene moieties on a subnanometer-sized Pt cluster surface. TBAP=tetra-*n*-butylammonium perchlorate.



Platinum Nanoparticles

P. Hu, L. Chen, C. P. Deming, X. Kang, S. Chen* 1455–1459

Nanoparticle-Mediated Intervalence Charge Transfer: Core-Size Effects

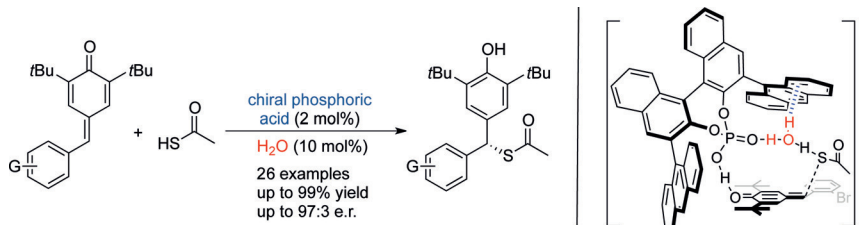


Organocatalysis

N. Dong, Z.-P. Zhang, X.-S. Xue, X. Li,*
J.-P. Cheng 1460 – 1464



Phosphoric Acid Catalyzed Asymmetric
1,6-Conjugate Addition of Thioacetic Acid to
para-Quinone Methides



Building bridges: The title reaction was realized in the presence of water, and successfully solved the challenge of remote stereocontrol for the *para*-quinone methide substrates. Theoretical studies indicated that the water-bridged proton

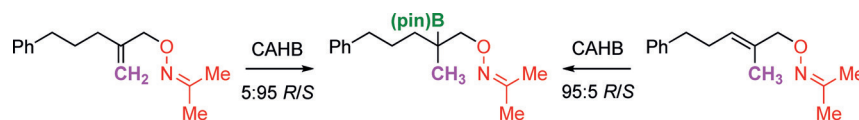
transfer and an unprecedented O—H... π interaction, between water and the aromatic nucleus of the chiral phosphoric acid, play important roles in the transition state.

Asymmetric Catalysis

V. M. Shoba, N. C. Thacker, A. J. Bochat,
J. M. Takacs* 1465 – 1469



Synthesis of Chiral Tertiary Boronic Esters
by Oxime-Directed Catalytic Asymmetric
Hydroboration



Take a CAHB, but give good directions: Methylidene and trisubstituted alkene substrates were converted into chiral tertiary boronic esters (up to 87% yield and 96:4 e.r.) by oxime-directed catalytic asymmetric hydroboration (CAHB) with

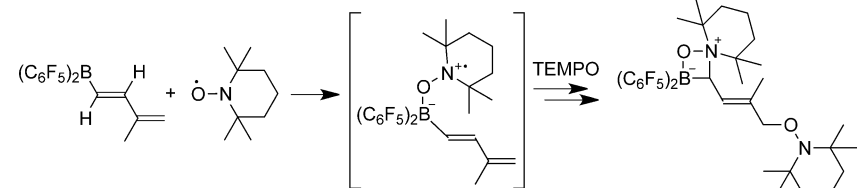
a simple rhodium catalyst. Subsequent C—C coupling to form a quaternary stereocenter was demonstrated, as well as other transformations to give a chiral diol, O-substituted hydroxylamine, or isoxazoline.

Nitroxide Radicals

F. Tükyilmaz, G. Kehr, J. Li, C. G. Daniliuc,
M. Tesch, A. Studer,*
G. Erker* 1470 – 1473



Selective N,O-Addition of the TEMPO
Radical to Conjugated Boryldienes



Things that go BONC... B(C₆F₅)₂-substituted dienes reacted with two molar equivalents of tetramethylpiperidine-1-oxyl (TEMPO) to give N,O-addition products containing a B,O,N,C four-membered

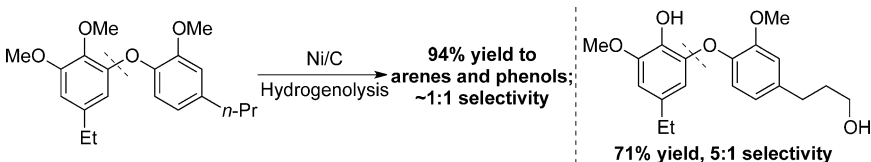
heterocyclic ring (see example). The reaction is thought to involve the addition of TEMPO to the boron atom to give an N-centered radical that then undergoes rapid C—N bond formation.

C—O Bond Cleavage

F. Gao, J. D. Webb,
J. F. Hartwig* 1474 – 1478

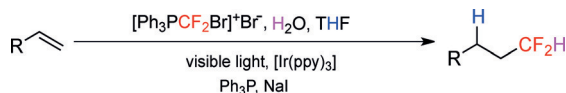


Chemo- and Regioselective
Hydrogenolysis of Diaryl Ether C—O
Bonds by a Robust Heterogeneous Ni/C
Catalyst: Applications to the Cleavage of
Complex Lignin-Related Fragments



Nick's pillar of strength: A catalyst comprising heterogeneous nickel particles supported on activated carbon promoted the efficient chemo- and regioselective hydrogenolysis of C—O bonds in di-*ortho*-substituted diaryl ethers to give arenes

and phenols without hydrogenation (see scheme). The high thermal stability of the embedded metal particles enabled C—O bond cleavage to occur in highly substituted diaryl ether units akin to those in lignin.



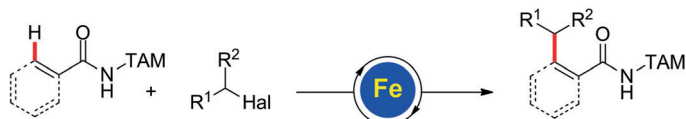
Getting involved: The visible-light photoredox catalysis of alkenes with a bromodifluoromethylphosphonium bromide using H₂O and THF as hydrogen sources afforded hydrodifluoromethylated alkanes

in moderate to excellent yields. The in situ generated difluoromethylphosphonium salt and a CF₂H radical are involved in this transformation. ppy = 2-phenylpyridine.

Photochemistry

Q.-Y. Lin, X.-H. Xu, K. Zhang,
F.-L. Qing* 1479–1483

Visible-Light-Induced Hydrodifluoromethylation of Alkenes with a Bromodifluoromethylphosphonium Bromide



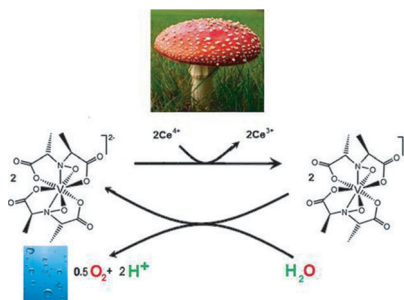
One for all: A unified strategy for iron-catalyzed C–H allylation and alkylation was developed by the use of a triazole directing group that could be cleaved under exceedingly mild conditions. The

inexpensive catalyst promotes the site-selective functionalization of arenes, heteroarenes, and alkenes with a wide range of primary and secondary allyl and alkyl groups.

Iron Catalysis

G. Cera, T. Haven,
L. Ackermann* 1484–1488

Expedient Iron-Catalyzed C–H Allylation/Alkylation by Triazole Assistance with Ample Scope

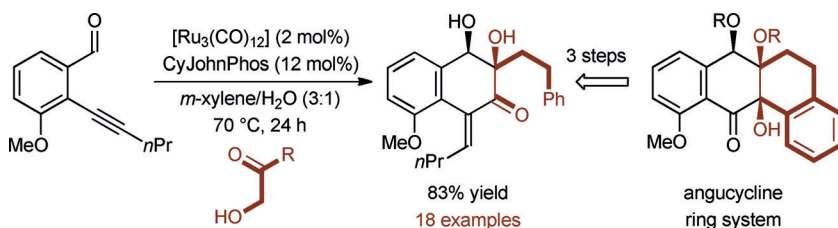


Kept in the dark: Amavadin and related vanadium complexes are shown to be capable of promoting water oxidation under non-photochemical conditions through a mechanism involving cooperation between the mononuclear metal center and ligands.

Transition-Metal Catalysts

M. Domarus, M. L. Kuznetsov, J. Marçalo,
A. J. L. Pombeiro,*
J. A. L. da Silva* 1489–1492

Amavadin and Homologues as Mediators of Water Oxidation



Ringling with efficiency: Ruthenium(0) complexes modified by either CyJohnPhos or RuPhos catalyze the successive C–C coupling of acetylenic aldehydes with α -ketols to form [4+2] cycloadducts as

single diastereomers. This method enables convergent construction of type II polyketide ring systems of the angucycline class.

Cycloaddition

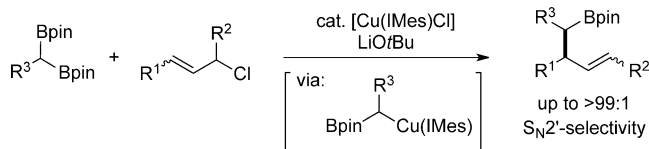
A. Saxena, F. Perez,
M. J. Krische* 1493–1497

Ruthenium(0)-Catalyzed [4+2] Cycloaddition of Acetylenic Aldehydes with α -Ketols: Convergent Construction of Angucycline Ring Systems



Allylic Compounds

J. Kim, S. Park, J. Park,
S. H. Cho* — 1498 – 1501



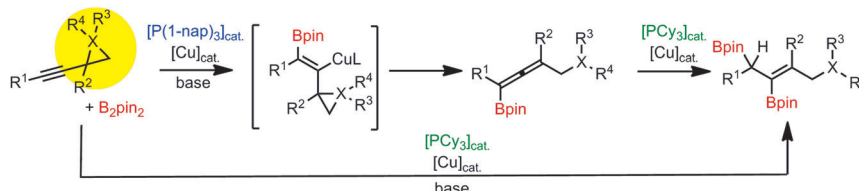
Synthesis of Branched Alkylboronates by Copper-Catalyzed Allylic Substitution Reactions of Allylic Chlorides with 1,1-Diborylalkanes

Readily accessible 1,1-diborylalkanes are used as the alkyl source in the title reaction. The method has a wide substrate scope, is highly regioselective for the S_N2'

product. IMes = 1,3-bis(2,4,6-trimethylphenyl)imidazole-2-ylidene, pin = pinacolato.

Homogeneous Catalysis

J. Zhao, K. J. Szabó* — 1502 – 1506



Catalytic Borylative Opening of Propargyl Cyclopropane, Epoxide, Aziridine, and Oxetane Substrates: Ligand Controlled Synthesis of Allenyl Boronates and Alkenyl Diboronates

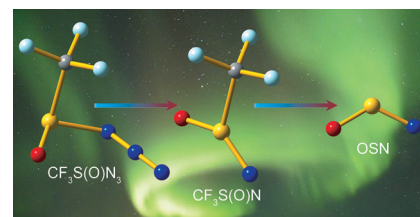
Strain-breaking: A copper-catalyzed reaction for the stereo- and regioselective synthesis of alkenyl diboronates and allenyl boronates is presented. In this process propargyl derivatives of strained three/four-membered rings were

employed as substrates and B_2pin_2 was used as the boronate source. Selective formation of the alkenyl diboronate versus the allenyl boronate products was controlled by the choice of phosphine ligand.

IR Spectroscopy

Z. Wu, D. Q. Li, H. M. Li, B. F. Zhu,
H. L. Sun, J. S. Francisco,
X. Q. Zeng* — 1507 – 1510

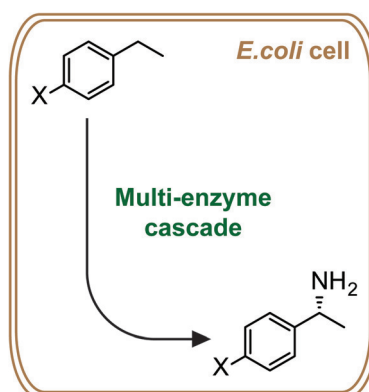
The triatomic molecule OSN was generated from the stepwise decomposition of gaseous $CF_3S(O)N_3$ via the novel sulfinyl nitrene $CF_3S(O)N$. Matrix IR spectroscopy and DFT calculations were employed to identify and characterize the matrix-isolated decomposition products and to elucidate the reaction mechanism.



Gas-Phase Generation and Decomposition of a Sulfinylnitrene into the Iminyl Radical OSN

Biocatalysis

P. Both, H. Busch, P. P. Kelly, F. G. Mutti,
N. J. Turner, S. L. Flitsch* — 1511 – 1513

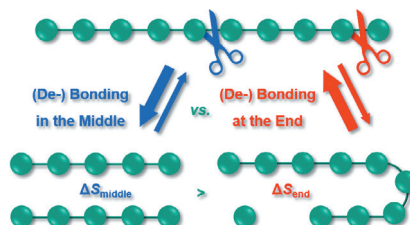


Whole-Cell Biocatalysts for Stereoselective C–H Amination Reactions

Enantiomerically pure chiral amines are ubiquitous chemical building blocks in bioactive pharmaceuticals and their synthesis from simple starting materials is of great interest. One strategy is the stereoselective installation of a chiral amine through formal C–H amination. A multi-enzyme cascade was constructed and applied in a single bacterial whole cell that can catalyze stereoselective benzylic aminations with 97.5% *ee*.

Inside Cover

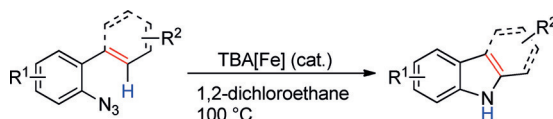
Middle versus end? When all other conditions are equal, bond cleavage in the middle of molecules is entropically much more favored than bond cleavage at the end. Experimental and theoretical approaches were used to study the selectivity of bond cleavage or dissociation of both covalent and supramolecular adducts. The findings have extensive implications for other fields of chemistry.



Polymer Chain Cleavage

K. Pahnke, J. Brandt, G. Gryn'ova,
C. Y. Lin, O. Altintas, F. G. Schmidt,
A. Lederer,* M. L. Coote,*
C. Barner-Kowollik* — 1514–1518

Entropy-Driven Selectivity for Chain
Scission: Where Macromolecules Cleave



The nucleophilic iron complex

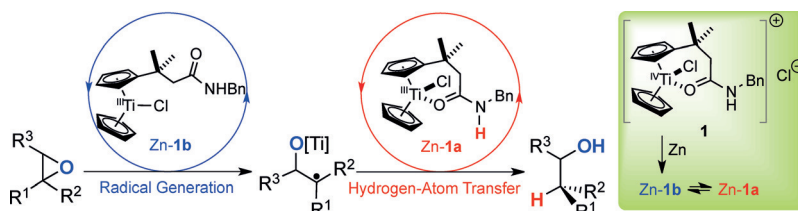
$\text{Bu}_4\text{N}[\text{Fe}(\text{CO})_3(\text{NO})]$ (TBA[Fe]) catalyzes the selective intramolecular aryl/vinyl $\text{C}(\text{sp}^2)\text{--H}$ amination of aryl azides to give either substituted carbazole or indole

derivatives in good to excellent yields. Kinetic isotope effects reveal a mechanistic similarity to the non-catalyzed thermal and rhodium-catalyzed variants.

Heterocycle Synthesis

I. T. Alt, B. Plietker* — 1519–1522

Iron-Catalyzed Intramolecular $\text{C}(\text{sp}^2)\text{--H}$
Amination



It takes two to tango: The coupling of catalytic cycles to enable the activation of amide N--H bonds for radical reduction is reported. This can either be achieved by using a bifunctional amide-substituted

catalyst or through cooperative catalysis with amide-substituted titanocenes and Crabtree's catalyst. The results lead the way for the use of peptides in HAT catalysis.

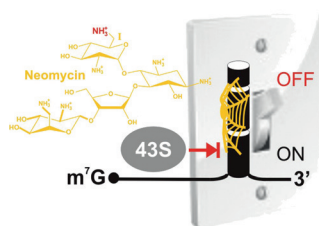
Radical Catalysis

Y.-Q. Zhang, V. Jakoby, K. Stainer,
A. Schmer, S. Klare, M. Bauer, S. Grimme,
J. M. Cuerva, A. Gansäuer* — 1523–1526

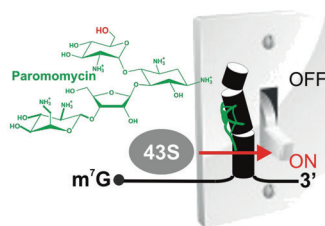
Amide-Substituted Titanocenes in
Hydrogen-Atom Transfer Catalysis



Front Cover



Think local, act global: A synthetic neomycin riboswitch also binds paromomycin, which differs from neomycin only in the substitution of an amino group with a hydroxy group. Binding of paromomycin does not activate the switch, however,



because the loss of key intermolecular interactions at one position of the paromomycin complex is translated through a defined network of intramolecular interactions into global changes in RNA conformational dynamics.

Riboswitches

E. Duchardt-Ferner,
S. R. Gottstein-Schmidtke, J. E. Weigand,
O. Ohlenschläger, J.-P. Wurm,
C. Hammann, B. Suess,
J. Wöhnert* — 1527–1530

What a Difference an OH Makes:
Conformational Dynamics as the Basis for
the Ligand Specificity of the Neomycin-
Sensing Riboswitch



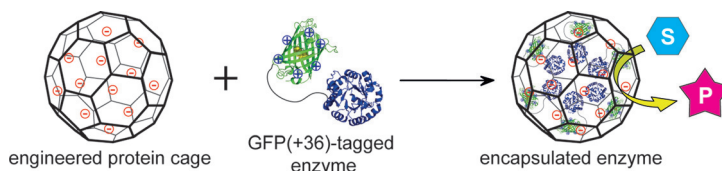


Nanoreactors

Y. Azuma, R. Zschoche, M. Tinzl,
D. Hilvert* 1531 – 1534



Quantitative Packaging of Active Enzymes
into a Protein Cage



Caught in a trap: Genetic fusion of cargo proteins to a positively supercharged variant of green fluorescent protein enables their quantitative encapsulation by

engineered lumazine synthase capsids possessing a negatively charged luminal surface.

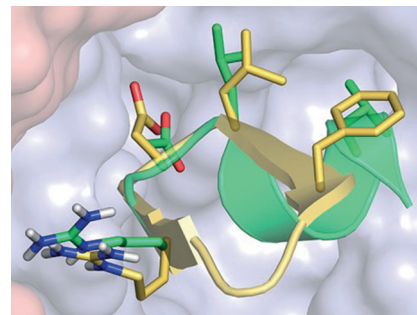
Integrin Ligands (1)

O. V. Maltsev, U. K. Marelli, T. G. Kapp,
F. S. Di Leva, S. Di Maro, M. Niebler,
U. Reuning, M. Schwaiger, E. Novellino,
L. Marinelli, H. Kessler* 1535 – 1539



Stable Peptides Instead of Stapled
Peptides: Highly Potent $\alpha\beta 6$ -Selective
Integrin Ligands

The search for binding: The $\alpha\beta 6$ integrin binds the RGD-containing peptide of the foot and mouth disease virus with high selectivity. The long binding helix of this ligand was downsized to an enzymatically stable cyclic peptide endowed with sub-nanomolar binding affinity toward the $\alpha\beta 6$ receptor and remarkable selectivity against other integrins.

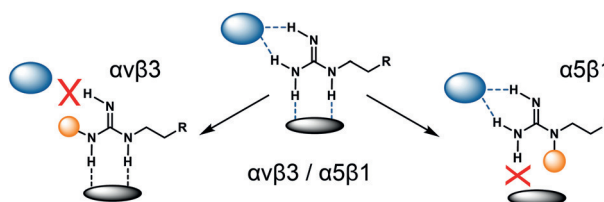


Integrin Ligands (2)

T. G. Kapp, M. Fottner, O. V. Maltsev,
H. Kessler* 1540 – 1543



Small Cause, Great Impact: Modification
of the Guanidine Group in the RGD Motif
Controls Integrin Subtype Selectivity



Simple modification of the guanidine group of the integrin ligand cilengitide can be used to tune integrin subtype selectivity in two directions. The two isomeric

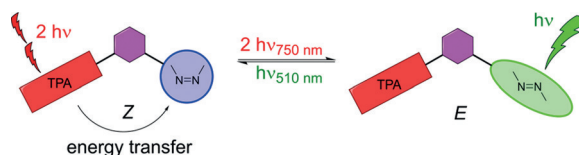
compounds obtained vary only in the position of a guanidine methyl group but have completely opposite selectivity properties for $\alpha\beta$ and $\alpha 5$ integrins.

Photoswitches

J. Moreno, M. Gerecke, L. Grubert,
S. A. Kovalenko,* S. Hecht* 1544 – 1547

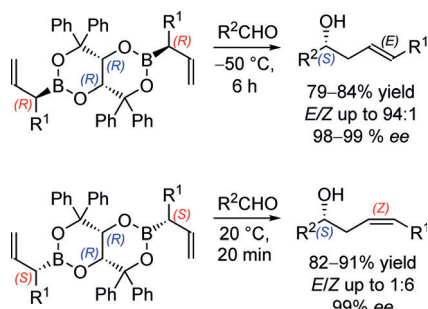


Sensitized Two-NIR-Photon $Z \rightarrow E$
Isomerization of a Visible-Light-
Addressable Bistable Azobenzene
Derivative



Red light, green light: Photoswitching with two NIR photons was accomplished by covalently linking a two-photon-harvesting triarylamine antenna (TPA) to

a thermally stable azobenzene derivative. The new photoswitch is addressable with visible and NIR light through one-photon and two-photon excitation, respectively.

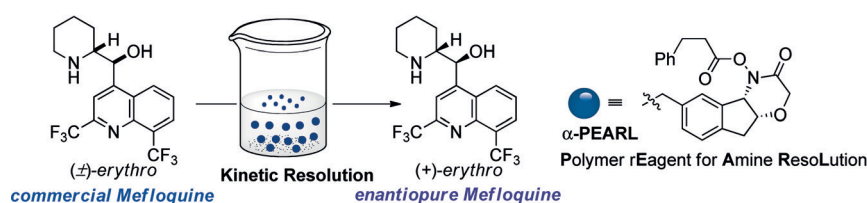


All isomers of homoallylic alcohols are readily accessible. The required enantiomerically pure allylboronates can be prepared by a short and convenient three-step sequence. The diboron compounds show unprecedented high reactivity. The observed selectivity as well as the relative reactivity were studied by computational methods.

Asymmetric Synthesis

M. Brauns, F. Muller, D. Glden, D. Bse, W. Frey, M. Breugst,*
J. Pietruszka* ————— **1548 – 1552**

Enantioselective Catalysts for the Synthesis of α -Substituted Allylboronates—An Accelerated Approach towards Isomerically Pure Homoallylic Alcohols



Pearl Jam: A novel ROMP-gel supported reagent allows the preparation of enantiopure (+)-*erythro*-mefloquine on a decagram scale from its racemate. The monomer synthesis does not require chromatographic purification, and polymeri-

zation can be carried out safely on a > 30 gram scale. PEARL is readily recovered after each cycle and has been applied for resolution of a broad range of N-heterocycles.

Kinetic Resolution

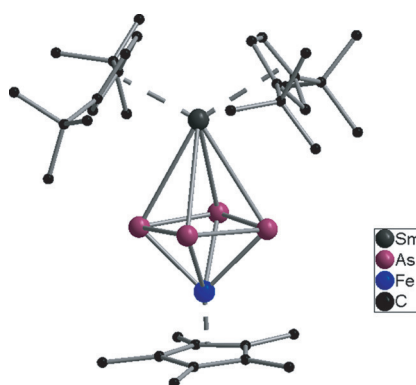
I. Kreituss, K.-Y. Chen, S. H. Eitel, J.-M. Adam, G. Wuitschik, A. Fettes, J. W. Bode* ————— **1553 – 1556**

A Robust, Recyclable Resin for Decagram Scale Resolution of (\pm)-Mefloquine and Other Chiral N-Heterocycles



Sandwich with arsenic filling:

$[(\text{Cp}''_2\text{Sm})(\mu, \eta^4: \eta^4\text{-As}_4)(\text{Cp}^*\text{Fe})]$ and $[(\text{Cp}''_2\text{Sm})_2\text{As}_7(\text{Cp}^*\text{Fe})]$, which are the first polyarsenides of the rare-earth metals, are reported. $[(\text{Cp}''_2\text{Sm})(\mu, \eta^4: \eta^4\text{-As}_4)(\text{Cp}^*\text{Fe})]$ is also the first d/f-triple decker sandwich complex with a purely inorganic aromatic middle deck.



Polyarsenides

N. Arleth, M. T. Gamer, R. Kppe, S. N. Konchenko, M. Fleischmann, M. Scheer, P. W. Roesky* — **1557 – 1560**

Molecular Polyarsenides of the Rare-Earth Elements



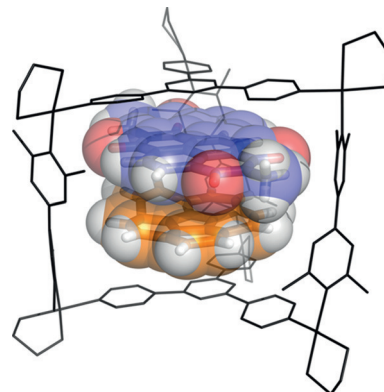
Host–Guest Systems

B. M. Schmidt, T. Osuga, T. Sawada,
M. Hoshino, M. Fujita* — 1561–1564



Compressed Corannulene in a Molecular Cage

Molecular compressor: Self-assembled coordination cages can compress the bowl-shaped guest corannulene when encapsulated in a pillared cage. Unsubstituted corannulene was pairwise included together with naphthalene diimide, while bromocorannulene formed a defined homodimer to be accommodated.



Supporting information is available on www.angewandte.org (see article for access details).



A video clip is available as Supporting Information on www.angewandte.org (see article for access details).



This article is available online free of charge (Open Access).



This article is accompanied by a cover picture (front or back cover, and inside or outside).



The Very Important Papers, marked VIP, have been rated unanimously as very important by the referees.



The Hot Papers are articles that the Editors have chosen on the basis of the referee reports to be of particular importance for an intensely studied area of research.

Angewandte Corrigendum

Synthesis of 3,4,5-Trisubstituted Isoxazoles from Morita–Baylis–Hillman Acetates by an NaNO_2/I_2 -Mediated Domino Reaction

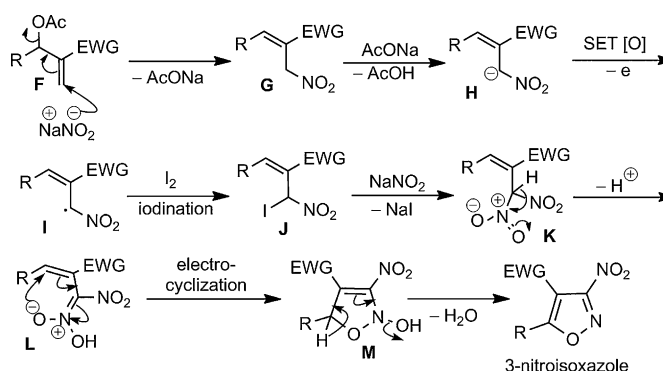
S. U. Dighe, S. Mukhopadhyay, S. Kolle,
S. Kanojiya, S. Batra* — 10926–10930

Angew. Chem. Int. Ed. 2015, 54

DOI: 10.1002/anie.201504529

In this Communication, the statement “analogous nucleophilic addition on the C–H bond α to the nitro group is unprecedented” (page 10927, first paragraph, line 6–7) must be retracted. The authors inadvertently omitted citing two seminal publications^[1,2] pertaining to oxidative nitration of nitroalkanes which were brought to their notice by an attentive reader.

In view of these publications, an alternate mechanism which appears to be more logical towards explaining the formation of the observed product is suggested (Scheme 3). This detail however has no bearing on the conclusions from the manuscript.



Scheme 3. Plausible mechanism for the transformation of MBH acetates into 3,4,5-trisubstituted isoxazoles. SET = single-electron transfer.

[1] N. A. Petrova, M. B. Shcherbinin, A. G. Bazanov, I. V. Tselinskii, *Russian J. Org. Chem.* 2007, 43, 640–651.

[2] K. Baum, D. A. Lerdal, J. S. Horn, *J. Org. Chem.* 1978, 43, 203–209.